Cell Cycle 13:20, 3241–3248; October 15, 2014; © 2014 Taylor & Francis Group, LLC

Temporal separation of replication and transcription during S-phase progression

Matthieu Meryet-Figuiere[1], Babak Alaei-Mahabadi[2], Mohamad Moustafa Ali[1], Sanhita Mitra[1], Santhilal Subhash[1], Gaurav Kumar Pandey[1], Erik Larsson[2,*], and Chandrasekhar Kanduri[1,*]

[1]Department of Medical Genetics; Institute of Biomedicine; The Sahlgrenska Academy; University of Gothenburg; Gothenburg, Sweden; [2]Department of Medical Biochemistry and Cell Biology; Institute of Biomedicine; The Sahlgrenska Academy; University of Gothenburg; Gothenburg, Sweden

Keywords: Cell cycle, Replication, Replication timing, S-phase, Transcription

Abbreviations: Ethynyl Uridine, EtU

Transcriptional events during S-phase are critical for cell cycle progression. Here, by using a nascent RNA capture assay coupled with high-throughput sequencing, we determined the temporal patterns of transcriptional events that occur during S-phase. We show that genes involved in critical S-phase-specific biological processes such as nucleosome assembly and DNA repair have temporal transcription patterns across S-phase that are not evident from total RNA levels. By comparing transcription timing with replication timing in S-phase, we show that early replicating genes show increased transcription late in S-phase whereas late replicating genes are predominantly transcribed early in S-phase. Global anti-correlation between replication and transcription timing was observed only based on nascent RNA but not total RNA. Our data provides a detailed view of ongoing transcriptional events during the S-phase of cell cycle, and supports that transcription and replication are temporally separated.

Introduction

Progression through the cell cycle is tightly regulated, and important insights about the cell cycle control machinery has been gained from global gene expression studies in eukaryotic cells, including yeast and human cell lines (HeLa, U2OS, foreskin fibroblasts).[1-4] The S-phase is a critical period of the cell cycle, where DNA replication needs to be coordinated with the expression of S-phase specific genes involved in nucleosome assembly, DNA replication and repair, and cell proliferation. Incorrect execution of these events can lead to genomic alterations and oncogenesis, and this has motivated studies of gene expression levels at different time points during S-phase.[5,6] However, in mammalian cells, the transcriptional events during S-phase are fast paced, as they all can occur during the course of 5–10 hours. It is therefore possible that total RNA levels, as measured in previous studies, will not provide sufficient detail. Transiently expressed RNAs may not reach measurable absolute RNA levels, or their precise transcriptional timing may be obscured by slow RNA decay at this time scale. We therefore hypothesized that measurements of nascent RNA levels, rather than absolute levels, may provide a more informative picture of transcriptional activity during the course of the S-phase.

One of the most intriguing aspects of S-phase is how the timing of DNA replication and gene transcription events is coordinated. It has been shown that co-temporal transcription and replication may lead to collisions between the replication machinery and transcriptional elongating complexes, which could be deleterious and accompanied by DNA damage and recombination.[7,8] Visualization of nascent DNA and RNA using fluorescence microscopy has suggested that replication and transcription are separated during S-phase in mammalian cells.[9] However, with the exception of a few selected loci, this has not been confirmed at global level using higher resolution methodologies. For example, in multicopy loci such as rDNA (rDNA) regions, transcription and replication are temporally separated.[10] Similar temporal separation has also been noted at the Cyclin B1 gene locus.[7,11] Given that these investigations were performed only on a handful of loci, or using low-resolution techniques, there is a need to determine the temporal coordination between replication and gene transcription during S-phase on a global scale.

We have adapted a nascent RNA capture assay to record ongoing transcriptional events at different time-points of the S-phase. By using this assay, we show that gene sets involved in several biological processes, including critical S-phase-specific functions such as nucleosome assembly and DNA repair, have temporal transcription patterns across S-phase that are not evident from total RNA levels. By comparing ongoing transcriptional events with replication timing across S phase, using both total and nascent RNA levels, we show that early replicating genes typically have their peak transcription in late S-phase, while late replicating genes are most strongly transcribed in early S-phase. This anti-correlation between replication and gene

*Correspondence to: Chandrasekhar Kanduri; Email: kanduri.chandrasekhar@gu.se; Erik Larsson; Email: erik.larsson@gu.se
Submitted: 05/16/2014; Revised: 08/06/2014; Accepted: 08/07/2014
http://dx.doi.org/10.4161/15384101.2014.953876

expression on a global scale was evident only using nascent RNA data but not total RNA, supporting that transcription and replication are temporally separated during S phase.

Results

Establishment of a nascent RNA capture assay to map transcriptional events during S phase

To gain insight into ongoing transcriptional events we captured and deep sequenced the nascent transcriptional output at 3 time points of the S-phase. To capture nascent transcription, we supplemented culture media with Ethynyl Uridine (EtU), a nucleoside analog of uracil that was incorporated into RNA during transcription. The Ethynyl group of EtU was tagged with a biotin moiety using the "Click It" chemistry reaction, performed on purified RNA or in situ on fixed cells. Then, biotinylated EtU-containing RNA molecules were affinity purified using streptavidin beads and deep sequenced. A flowchart describing the outline of labeling and purification protocol of EtU labeled RNAs is shown in **Figure 1A** (see Methods for detailed protocol).

We chose to synchronize HeLa cells at the beginning of S phase using a "double block" method, supplementing the culture media with thymidine followed by hydroxyurea. This method has been shown to perform better than other synchronization methods such as mitotic shake-off, serum starvation or contact inhibition, which may cause limited synchrony of cancer cells.[12,13] Since hydroxyurea exposure for longer times (more than 24 hours) can trigger cellular toxicity, fork collapse and

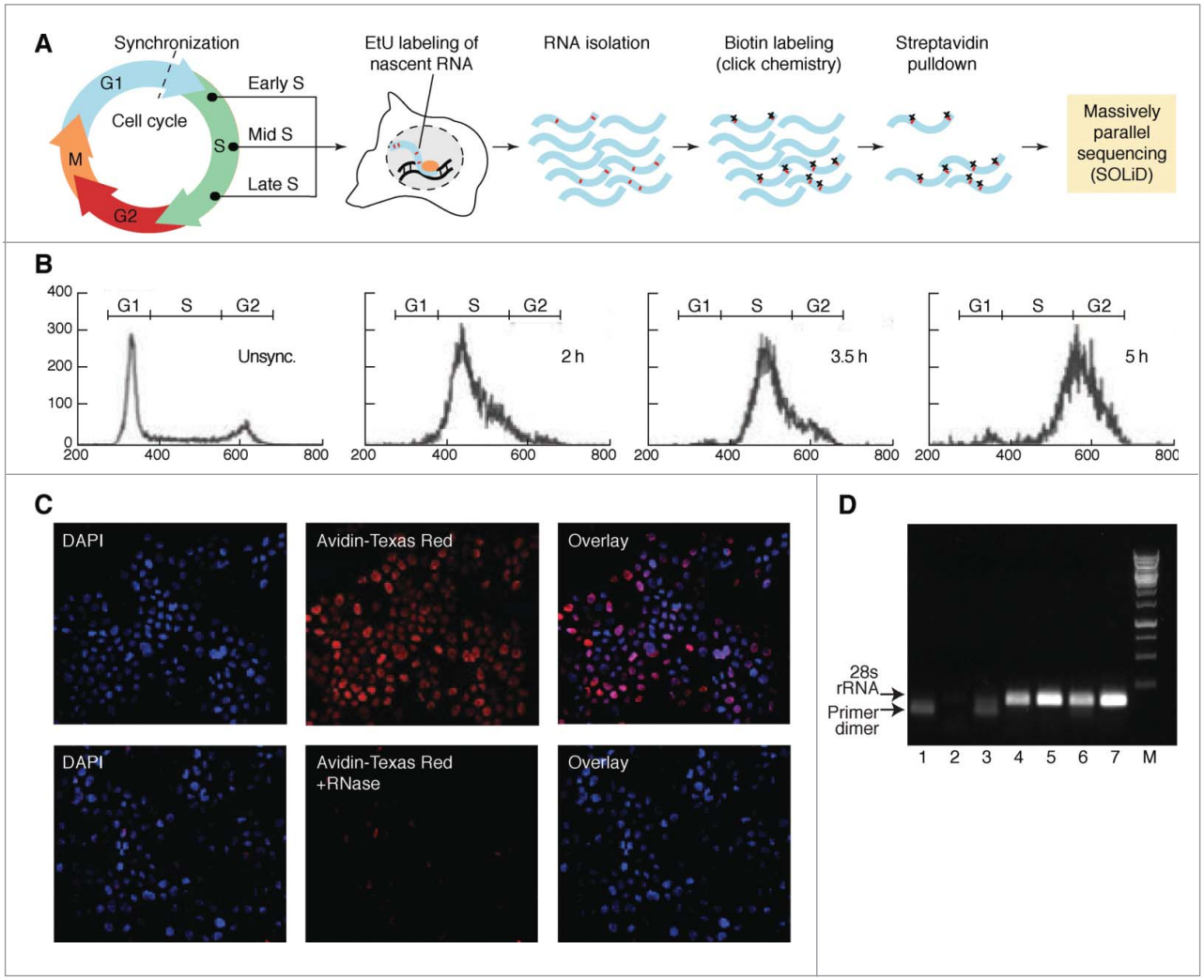

Figure 1. Isolation of nascent RNA at different stages of S-phase progression. (**A**) Flow chart describing the outline of the nascent RNA capture assay. Cells were synchronized and nascent RNA was isolated by pulsing cells with EtU at 3 timepoints of the S-phase. RNA was subjected to SOLiD sequencing. (**B**) Flow cytometry showing position of the cell population in cell cycle. Unsync: unsynchronized cells, 2 h, 3.5 h and 5 h: 2 hours, 3.5 hours and 5 hours after block release respectively. (**C**) EtU incorporation in RNA and not in DNA. Following EtU labeling and Click-IT reaction to add biotin moiety to EtU, the unsynchronized HeLa cells were immunostained using avidin coupled to Texas red (red color). Cell nuclei were stained with DAPI (blue color). (**D**) Pulldown is specific for EtU treated RNA. Agarose gel picture showing the semi-quantitative RT-PCR products of 28 s RNA. Lanes 1-3: non EtU treated HeLa cell RNA pull down. Lanes 4-6: EtU treated HeLa RNA pull down. Lane 7: control RNA (no pull down).

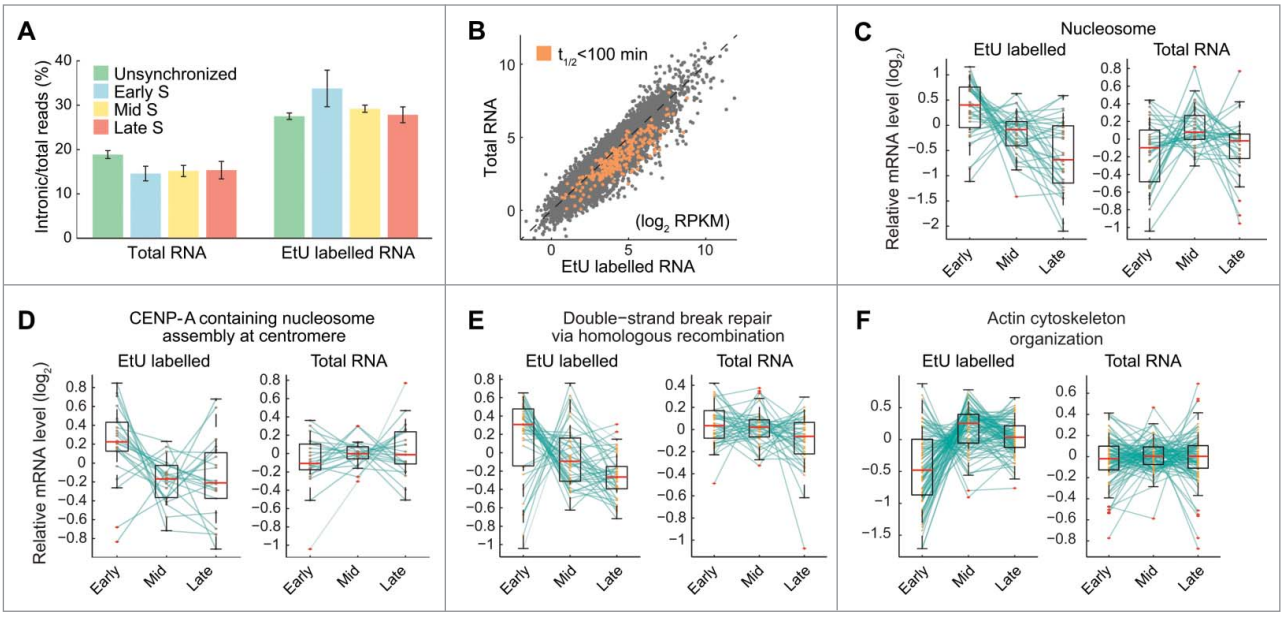

Figure 2. Temporal transcription patterns during HeLa S-phase determined using massively parallel sequencing. (**A**) Comparison of total RNA and EtU-labeled (nascent) RNA with respect to percentage intronic reads shows elevated intronic read coverage in the labeled data. Intronic and total read counts (intronic + exonic) were determined individually for all expressed genes (>20 reads). Bars show average percentages and error bars indicate +/− SEM. (**B**) Scatterplot of expression levels obtained based on nascent RNA (x-axis) and total RNA (y-axis), for individual expressed genes in unsynchronized cells (Pearson's r = 0.91). The majority of a set of 243 unstable mRNAs (half-live < 100 minutes, defined using available stability data[15]) showed reduced total RNA levels relative to their production rates (EtU labeled data). (**C–F**) Genes associated with nucleosome, CENP-A nucleosome and double strand break repair GO terms showed elevated transcription in early s-phase, as indicated by the EtU labeled data. Actin cytoskeleton-related genes showed peak transcription in mid S-phase. Levels were normalized relative to the mean expression of each gene across all time points. Box plots: bars correspond to the median and the central boxes span the middle quartiles. Green lines connect each gene throughout the time series. RPKM, reads-per-kilobase-per-million reads; t1/2, half-life.

double strand breaks in DNA, we limited hydroxyurea treatment to 12 hours, which has previously been shown to cause no such deleterious effects. [14] Consistently, we detected no cellular toxicity in our experiments (**Fig. 1B** and data not shown).

We compartmentalized S phase into 3 partly overlapping stages of 2 hours. "T0" denote the time point at which the cells were released from the cell cycle arrest. T0 cells are slightly inside S-phase, as our synchronizations method arrests the cells at the onset of S-phase. T5 represents the end of S-phase, as the DNA amount is doubled at this stage. Hence, T0-T2, T1.5-T3.5 and T3-T5.0 represent early, mid and late S stages of S-phase, respectively. Upon release from block, for each S phase stage, cells were grown in media containing EtU and were harvested at the end of the 2 hours labeling of nascent transcription. Position of the cell population during cell cycle was monitored by flow cytometry at each harvesting time point (**Fig. 1B**). Unsynchronized cells were used as a control. In addition, cell synchronization was also assessed by performing RT-qPCR on genes that have been shown to have periodic expression changes during early (CDC6) and late stages of S-phase (CCNB1) (**Fig. S1**).

We next verified incorporation of EtU into nascent RNA by immunocytochemistry using avidin coupled to Texas red on cells labeled with EtU for 2 hours followed by its biotinylation using click chemistry. The specificity of EtU incorporation into RNA, but not DNA, was confirmed by the disappearance of fluorescent signal after RNaseA treatment (**Fig. 1C**). We also repeated this experiment on cells synchronized at different stages of S-phase, and observed that the synchronization of cells did not impair EtU incorporation into nascent RNA (**Fig. S2**). We further verified the specificity of EtU labeled nascent RNA purification using 28 S rRNA as a target. For this purpose, we performed click chemistry to add biotin moieties to EtU labeled and unlabeled RNA and purified using streptavidin beads. 28S rRNA was detected by RT-PCR only from EtU-labeled RNA, but not from unlabeled total RNA, demonstrating that our purification protocol specifically purifies EtU-labeled RNA (**Fig. 1D**).

After verifying the specificity of our nascent RNA capture assay, we purified biotinylated EtU labeled RNA with streptavidin beads from early, mid and late stages of S-phase. In addition, unlabeled steady-state RNA matching the same stages of S-phase was isolated. Following rRNA depletion, the samples were subjected to deep sequencing and mapping to the human reference genome.

The nascent RNA assay captures temporal transcriptional events that are not revealed by total RNA levels

Nascent transcription implies ongoing transcriptional activity, and nascent RNA is therefore expected to contain relatively more intronic sequences while total RNA should contain more processed mRNA. Consistent with this, a higher proportion of sequencing reads were mapped to introns in EtU labeled RNA in comparison with the unlabeled total RNA (**Fig. 2A**). While the transcriptional profiles obtained using nascent RNA labeling

overall were strongly correlated with the total RNA profiles (r = 0.91) (**Fig. 2B**), there were still many differences at the level of individual genes (up to 30-fold) (**Fig. 2B**). Using available mRNA stability data from HeLa cells (Actinomycin D chase),[15] we found that mRNAs with short half-life consistently had reduced total RNA levels relative to their rate of production as indicated by the EtU data, supporting the levels obtained with the labeling protocol are biologically informative (**Fig. 2B**).

We next applied Gene Set Enrichment Analysis (GSEA) to the nascent RNA data, to identify gene categories that showed patterns of differential transcription across S-phase. Several gene ontology (GO) categories showed significant temporal changes in transcription (**Table S1**) including S phase-relevant categories such as histone genes ("nucleosome" set), CENP-A containing nucleosome assembly, and double-stranded break repair genes, all predominantly transcribed in early S-phase (**Fig. 2C-E**). Other categories, such as actin cytoskeleton organization genes, were predominantly transcribed in mid S-phase (**Fig. 2F**). Notably, these stage-specific patterns were often not evident in total RNA levels, suggesting that the effects were obscured by slow RNA decay (**Fig. 2C-F**). For example, in agreement with earlier data [5] we observed that total RNA levels of genes in the nucleosome category peaked in mid S phase, whereas in the labeled data, transcriptional activity of these genes was seen predominantly in the early S, indicating a gradual accumulation of these transcripts in mid S phase.

Taken together, our results suggest that our nascent capture assay records ongoing transcriptional events in S phase, and that it provides information about these events that are not revealed by total RNA levels.

Replication and transcription timing are inversely correlated

Having established the nascent RNA capture assay, we next sought to use the obtained data to investigate the relationship between replication timing and transcriptional timing during S phase on a global scale. Genes were separated into early and late replicating sets based on available data from HeLa cells[16] and average expression patterns across the three time points were determined, using both total and nascent RNA levels. We found that both types of data confirmed earlier observations that late-replicating genes in general are expressed at lower levels compared to early-replicating genes (**Fig. 3A**).[17–19]

Based on total RNA levels, we observed no differences in the average temporal transcription patterns of early compared to late replicating genes (**Fig. 3A**). However, the nascent RNA data revealed an inverse relationship between transcription and replication, such that late replicating genes on average had their peak transcription in early S-phase and vice versa (**Fig. 3A**). We found that this relationship was highly consistent also at the level of individual genes (**Fig. 3B**).

We next scored genes based on their temporal expression patterns in S-phase, such that early-expressed genes would be

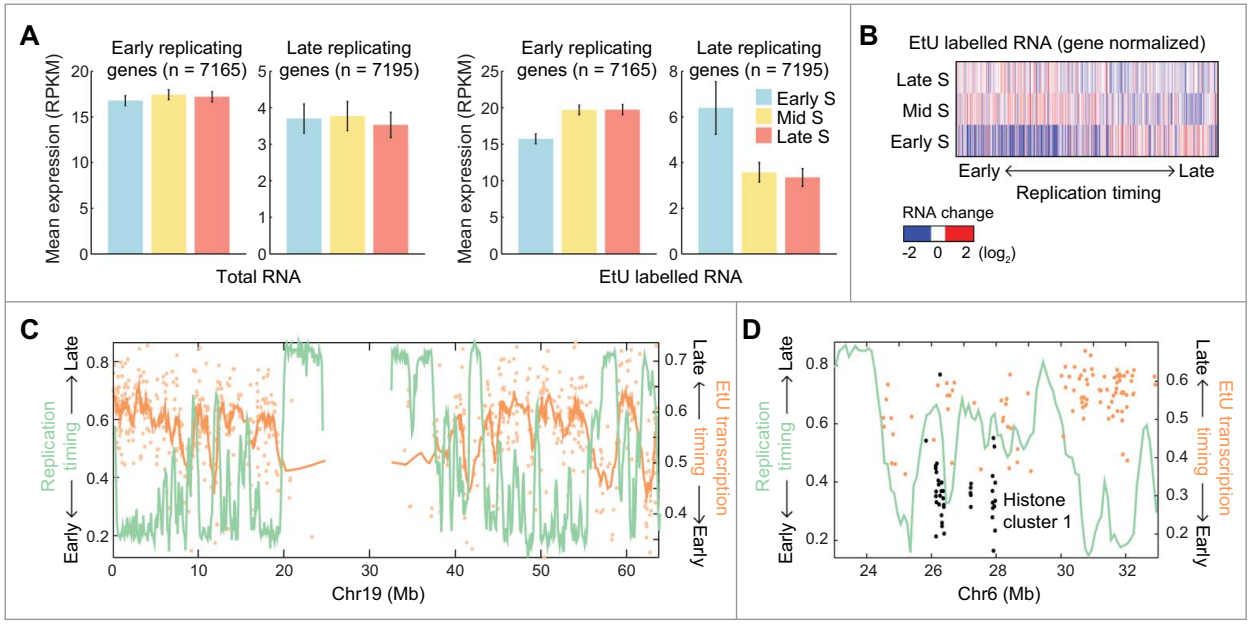

Figure 3. Relationship between replication timing and transcription during S-phase. (**A**) Late replicating genes on average show reduced transcription in late S-phase. Replication timing data from HeLa[16] was used to define sets of early and late replicating genes (lower and upper quartiles). Bars show average expression levels (+/− SEM) for these gene sets throughout S-phase. Results based on steady state RNA and EtU labeled nascent RNA are shown separately. (**B**) Heat map of relative EtU-based expression profiles for individual genes, ranked by their replication timing. Early replicating genes typically show lower expression levels in early compared to late S phase, and vice versa. Only expressed genes (minimum 20 reads in one time point) were considered. (**C**) Inverse relationship between replication and expression timing on chromosome 19. Expression patterns in S-phase were transformed into continuous scores reflecting the timing of expression (see **Fig. S3** and Methods). Expression timing for individual expressed genes is shown as light orange dots, while the darker orange line shows a moving average (n = 10 genes). (**D**) Detailed view of replication and expression timing near the HIST1 histone cluster on chromosome 6, with histone genes indicated in black.

assigned a low score and late-expressed genes would be assigned a high score (**Fig. S3** and Methods). This allowed us to investigate expression timing as a function of genomic position. We found that the strength of the inverse relationship between replication and transcription timing was variable between chromosomes (**Fig. S4A**), with chromosomes 19 (**Fig. 3C**) and 6 showing notable anti-correlation. We also found that the anti-correlation was somewhat more prominent for genes with strong S phase-specific expression (**Fig. S4B**). Early transcribed genes in histone cluster 1 on chromosome 6 were consistently late-replicating, while several closely positioned late-transcribed genes instead replicated early (**Fig. 3D**). In addition, using RT-qPCR we could confirm increased transcription in early S for several late-replicating genes in histone cluster 1 (**Fig. 4A**), and inversely late S phase increased transcription for several genes in early-replicating regions (**Fig. 4B**).

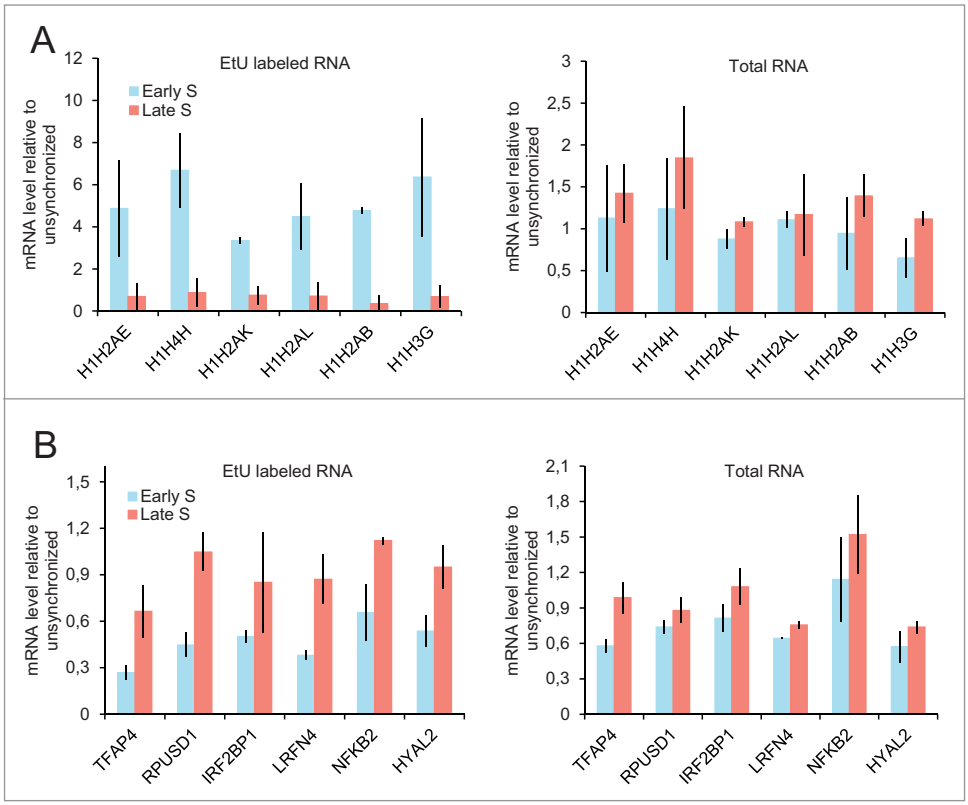

Figure 4. Inverse correlation between transcription and replication timing confirmed by RT-qPCR. (**A**) Nascent transcripts analysis show a higher transcription rate in early S-phase compared to late S-phase for late replicating genes, whereas total RNA does not. H1H2AE, H1H4H, H1H2AK, H1H2AL, H1H2AB and H1H3G histone genes are part of "nucleosome" gene set, and are located in histone cluster 1 on chromosome 6. (**B**) Nascent transcripts analysis show a higher transcription rate in late S-phase compared to early S-phase for early replicating genes, whereas total RNA does not. TFAP4, RPUSD1, IRF2BP1, LRFN4, NFKB2 and HYAL2 were randomly picked among the earliest replicating genes. (**A** and **B**) RNA from synchronized cells were EtU labeled, purified (see **Fig. 1A** and experimental procedures) and converted to cDNA. Total RNA from unlabeled cells were used as a control. Gene expression levels were measured by q-PCR and standardized with OCRL, which is expressed uniformly across S-phase in EtU and Total RNA according to sequencing data. Expression levels are relative to unsynchronized cells. Error bars represent standard deviation from 2 experiments.

Discussion

Using a nascent RNA capture assay we recorded the timing of transcriptional events during S-phase, and found that specific gene categories, such as nucleosome assembly, assembly of CENP containing nucleosomes DNA repair, and actin cytoskeleton organization show distinct temporal transcription patterns. This stage-specific expression was not evident based on total RNA levels, consistent with the idea that transcriptional events during S-phase are too fast-paced to be accurately reflected in the absolute RNA levels. Thus our nascent capture assay pinpoints accurate time points for transcriptional activation during S-phase, and also, reveal the highly dynamic nature of transcriptional events in this phase of the cell cycle.

When comparing the timing of transcription in relation to replication during S phase, we have shown that these 2 variables are inversely correlated: early replicating genes are more strongly transcribed late in S phase and late replicating genes are preferably transcribed in early S phase. This relationship was only visible when considering nascent RNA levels, indicative of transcription rates.

Collisions between transcription and replication complexes often result in replication fork stalling, followed by DNA damage and repair.[20] To evade these collisions, diverse mechanisms have evolved across evolutionary spectrum to separate the timing of transcription and replication.[21] For example, a recent global investigation in yeast has mapped the most frequent sites of replication fork pausing to highly transcribed genes, indicating that the process of transcription could negatively regulate fork migration.[22] Moreover, investigations on a few selected loci also support that replication and transcription may be temporally distinct during S phase: In the case of rDNA clusters, active rDNA copies replicate early and during ongoing replication they remain transcriptionally silent. Their transcription, however, is activated once the replication process is complete.[10,23] Similar temporal separation between replication and gene expression was also noted in case of single copy gene Cyclin B1, which is transcribed in late S-phase but replicated during early S-phase.[7] These individual examples are intriguing, but a high-resolution genome-wide analysis has been missing. Thus, our data provides a global view of the timing of transcriptional events during

S-phase and contributes to our understanding of the relationship between replication and transcription.

Methods

Cell culture and G1/S cell block

HeLa cells were cultured in MEM media (Gibco) supplemented with 10% FBS (Gibco), 4 mM glutamine (Sigma) and antibiotics (penicillin and streptomycin, Gibco), at 37°C in humidified atmosphere with 5% CO_2. For cell synchronization at the onset of S-phase of the cell cycle, HeLa cells were plated at 35% confluency and incubated for 10 hours in media supplemented with 2 mM thymidine (Sigma), washed in PBS and incubated in media supplemented with 1 mM hydroxyurea (Sigma) for 12 hours. Cells were released from block by washing in PBS and incubation in fresh media.

For the labeling of nascent transcripts, cells were incubated for 2 hours in media supplemented with 1 mM Ethynyl Uridine (Invitrogen). At designated time points, cells with or without EtU labeling were detached from plates with trypsin, washed in PBS, and either re-suspended in 70% ethanol (for flow cytometry), transferred on a microscope slide with a cytospin centrifuge (for in situ fluorescence) or subjected to RNA extraction (for deep sequencing).

Flow cytometry

100 000 cells stored at – 20°C in 70% ethanol were re-suspended in PBS, incubated at 37°C for 30 min, and then in 1 ml of DNA staining solution (200 ug/ml RNaseA and 50 ug/ml propidium iodide (Invitrogen) in PBS) for 2 hours at 4°C. DNA content was analyzed on a Eclipse flow cytometer (iCyt).

In situ fluorescence

Cells transferred to a microscope slide by cytospin centrifugation were fixed in 3,7% formaldehyde in PBS for 30 min. Slides were washed in PBS and fixation was quenched by incubating in 0,1 M glycine in PBS for 30 min. Cells were permeabilized with 0,1% Triton X 100 in PBS (PBS-T) for 10 min followed by blocking in PBS-T with 1% BSA for 1 hour. EtU containing RNA was biotinylated by a "Click It" chemistry reaction with Click It Cell Reaction Buffer Kit (Invitrogen) according to the manufacturer's protocol. Biotinylated EtU was detected using Avidin coupled with Texas Red (Vector labs) at a 1:500 dilution in PBS-T with 1% BSA for 30 min. Nuclei were stained with DAPI solution (100 μg/ml in PBS) and the slides were mounted with Vectashield Hard Set Mounting Medium (Vector Labs). When applicable, RNaseA digestion was performed before blocking with 400 μg/ml RNaseA in PBS for 1 h at 37°C.

Total RNA purification and reverse transcription (RT)

Total RNA were extracted at the designated time points in cell cycle with SV Total RNA Isolation System (Promega). For qPCR, 1 μg RNA was converted into cDNA with Superscript II Reverse Transcriptase (Invitrogen), and Q-PCR was performed with Go-Taq qPCR Master Mix (Promega) on a Step One Plus device (Applied biosystems) for 40 cycles (95°C, 15 sec; 55°C, 30 sec; 72°C, 30 sec). Primer sequences are listed in **Table S2**.

For deep-sequencing, RNA concentration was measured with Nanodrop and integrity was assessed on Bioanalyzer 2100 (Agilent) using RNA 6000 pico kit (Agilent), according to the manufacturer's protocol. For each time point, RNA from 2 independent experiments were pulled into 1 sample and deep-sequenced on SOLID sequencing platform at Uppsala Genome Center.

Nascent RNA purification and reverse transcription (RT)

EtU labeled nascent RNA were extracted at the designated time points in cell cycle with Tri reagent (Ambion). We performed DNA digestion with RQ1 DNase I (Promega) and re-extracted RNA with Tri reagent.

For semi quantitative PCR, RNA were subjected to biotinylation and purified on streptavidin beads using Click-It Nascent RNA Capture kit (Invitrogen). RT was performed directly on beads with Superscript II Reverse Transcriptase. cDNA-containing supernatant was used as template to perform PCR amplification with iproof High Fidelity enzyme (Biorad). PCR was performed for 40 cycles (95°C, 15 sec; 55°C, 30 sec; 72°C, 30 sec). PCR products were separated on 1% agarose gel stained with Sybr Safe (1:10 000, Invitrogen). For the experiment in **Figure. 1D**, unlabeled RNA were submitted to the above-described process. Primer sequences are listed in **Table S2**.

For deep sequencing and q-PCR, rRNA were first depleted from 10 ug input RNA with Ribominus Eukaryote kit (Invitrogen). rRNA-depleted RNA (2-3 ug per sample) were biotinylated.and purified on 50 ul streptavidin magnetic beads with Click-It Nascent RNA Capture kit (Invitrogen). Biotinylated RNA were eluted from the beads and fragmented by heating at 95°C for 3 min in 200 ul of a buffer containing 2 mM biotin, 1 M NaCl, 50 mM MOPS, 5 mM EDTA, 2 M β mercapto ethanol, pH 7,4. Supernatant (200 ul) containing eluted RNA was recovered immediately after heating and RNA were precipitated in 30 ul 3 M Sodium Acetate (PH 5.2), 1 ul Glycoblue (Invitrogen), 750 ul Ethanol overnight at −20°C. For Q-PCR, purified RNA was converted into cDNA with Superscript II Reverse Transcriptase (Invitrogen) and q-PCR was performed with Go-Taq qPCR Master Mix (Promega) on a Step One Plus device (Applied biosystems) for 40 cycles (95°C, 15 sec; 55°C, 30 sec; 72°C, 30 sec). Primer sequences are listed in **Table S2**. For deep-sequencing, size distribution of purified RNA was assessed on a Bioanalyzer 2100 (Agilent) using RNA 6000 pico kit (Agilent) and RNA concentration was measured on a Qubit 2.0 fluorometer (Invitrogen). For each time point, RNA from 2 independent experiments were pulled into 1 sample and deep-sequenced on SOLID sequencing platform at Uppsala Genome Center.

RNA-seq analysis

Sequences were aligned to the human hg19 assembly using LifeScope. We used HTSeq-count (http://www-huber.embl.de/users/anders/HTSeq) in "intersection-strict" mode and using a

minimum alignment quality cutoff of 10, to derive gene-level counts based on the GENCODE V11 gene annotation, obtained through the UCSC browser. We considered 30418 coding genes and lncRNA genes that were all uniquely mapped to a single genomic locus. Between 4.3 and 12.2 (average 8.31) million GENCODE-mapped reads were obtained per library. RPKM-type expression levels were calculated by normalizing for mRNA length and library size as determined by the number of GENCODE-mapped reads. Quantifications of intronic vs. exonic reads were obtained by generating custom annotation files where each gene was represented as one large block that also included all associated intronic regions.

Available mRNA stability data in the form of Actinomycin D chase data from HeLa [15] was analyzed as described previously,[24] and a set of 243 genes with low half-lives (<100 minutes) was defined. Expression timing scores for individual genes, T, were determined using the following formula, where E, M and L are normalized expression values in early, mid and late S-phase, respectively: $T = L + M/(2*(E+M+L))$. The results of this function will vary between 0 (early S-specific expression) and 1 (late S-specific expression), with intermediate values awarded for mid or uniform expression.

We used the "preranked" module of GSEA [25,26] to identify gene categories that showed patterns of differential expression across S-phase. We considered gene sets with at least 5 and at most 150 genes from GO annotation files (GOC Validation Date: 01/22/2014) in the Gene Ontology database,[27] and differential expression ranked lists were made by comparing early and mid S-phase, early and late S-phase, and mid and late S-phase. Gene sets that reached significance at a false discovery rate (FDR) < 0.05 in minimum one comparison are listed in **Table S1**.

Disclosure of Potential Conflicts of Interest

No potential conflicts of interest were disclosed.

Acknowledgments

We thank Uppsala Genome Center and Science for Life Laboratory, Uppsala for high-throughput sequencing.

Funding

This work was supported by the grants from the Swedish Cancer Research foundation (Cancerfonden: Kontrakt no. 100422), Swedish Research Council (VR-M: K2014-67X-20781-07-4), Barncancerfonden (PR2013-0048), and LUA/ALF to CK.

References

1. Whitfield ML, Sherlock G, Saldanha AJ, Murray JI, Ball CA, Alexander KE, Matese JC, Perou CM, Hurt MM, Brown PO, et al. Identification of genes periodically expressed in the human cell cycle and their expression in tumors. Mol biol Cell 2002; 13:1977-2000; PMID:12058064; http://dx.doi.org/10.1091/mbc.02-02-0030
2. Grant GD, Brooks L, 3rd, Zhang X, Mahoney JM, Martyanov V, Wood TA, Sherlock G, Cheng C, Whitfield ML. Identification of cell cycle-regulated genes periodically expressed in U2OS cells and their regulation by FOXM1 and E2F transcription factors. Mol biol Cell 2013; 24:3634-50; PMID:24109597; http://dx.doi.org/10.1091/mbc.E13-05-0264
3. Cho RJ, Huang M, Campbell MJ, Dong H, Steinmetz L, Sapinoso L, Hampton G, Elledge SJ, Davis RW, Lockhart DJ. Transcriptional regulation and function during the human cell cycle. Nat Genet 2001; 27:48-54; PMID:11137997
4. Oliva A, Rosebrock A, Ferrezuelo F, Pyne S, Chen H, Skiena S, Futcher B, Leatherwood J. The cell cycle-regulated genes of Schizosaccharomyces pombe. PLoS Biol 2005; 3:e225; PMID:15966770
5. van der Meijden CM, Lapointe DS, Luong MX, Peric-Hupkes D, Cho B, Stein JL, van Wijnen AJ, Stein GS. Gene profiling of cell cycle progression through S-phase reveals sequential expression of genes required for DNA replication and nucleosome assembly. Cancer Res 2002; 62:3233-43; PMID:12036939
6. Sadasivam S, Duan S, DeCaprio JA. The MuvB complex sequentially recruits B-Myb and FoxM1 to promote mitotic gene expression. Genes Dev 2012; 26:474-89; PMID:22391450; http://dx.doi.org/10.1101/gad.181933.111
7. Helmrich A, Ballarino M, Tora L. Collisions between replication and transcription complexes cause common fragile site instability at the longest human genes. Mol Cell 2011; 44:966-77; PMID:22195969; http://dx.doi.org/10.1016/j.molcel.2011.10.013
8. Srivatsan A, Tehranchi A, MacAlpine DM, Wang JD. Co-orientation of replication and transcription preserves genome integrity. PLoS genetics 2010; 6: e1000810; PMID:20090829; http://dx.doi.org/10.1371/journal.pgen.1000810
9. Wansink DG, Manders EE, van der Kraan I, Aten JA, van Driel R, de Jong L. RNA polymerase II transcription is concentrated outside replication domains throughout S-phase. J Cell Sci 1994; 107(Pt 6):1449-56; PMID:7962188
10. Dimitrova DS. DNA replication initiation patterns and spatial dynamics of the human ribosomal RNA gene loci. J Cell Sci 2011; 124:2743-52; PMID:21807939; http://dx.doi.org/10.1242/jcs.082230
11. Helmrich A, Ballarino M, Nudler E, Tora L. Transcription-replication encounters, consequences and genomic instability. Nat Struct Mol Biol 2013; 20:412-8; PMID:23552296; http://dx.doi.org/10.1038/nsmb.2543
12. Davis PK, Ho A, Dowdy SF. Biological methods for cell-cycle synchronization of mammalian cells. BioTechniques 2001; 30:1322-6, 8, 30-1.
13. Fox MH, Read RA, Bedford JS. Comparison of synchronized Chinese hamster ovary cells obtained by mitotic shake-off, hydroxyurea, aphidicolin, or methotrexate. Cytometry 1987; 8:315-20; PMID:3109858; http://dx.doi.org/10.1002/cyto.990080312
14. Petermann E, Orta ML, Issaeva N, Schultz N, Helleday T. Hydroxyurea-stalled replication forks become progressively inactivated and require two different RAD51-mediated pathways for restart and repair. Molecular Cell 2010; 37:492-502; PMID:20188668; http://dx.doi.org/10.1016/j.molcel.2010.01.021
15. Iwamoto F, Stadler M, Chalupnikova K, Oakeley E, Nagamine Y. Transcription-dependent nucleolar cap localization and possible nuclear function of DExH RNA helicase RHAU. Exp Cell Res 2008; 314:1378-91; PMID:18279852; http://dx.doi.org/10.1016/j.yexcr.2008.01.006
16. Chen CL, Rappailles A, Duquenne L, Huvet M, Guilbaud G, Farinelli L, Audit B, d'Aubenton-Carafa Y, Arneodo A, Hyrien O, et al. Impact of replication timing on non-CpG and CpG substitution rates in mammalian genomes. Genome Res 2010; 20:447-57; PMID:20103589; http://dx.doi.org/10.1101/gr.098947.109
17. Lawrence MS, Stojanov P, Polak P, Kryukov GV, Cibulskis K, Sivachenko A, Carter SL, Stewart C, Mermel CH, Roberts SA, et al. Mutational heterogeneity in cancer and the search for new cancer-associated genes. Nature 2013; 499:214-8; PMID:23770567; http://dx.doi.org/10.1038/nature12213
18. Woodfine K, Fiegler H, Beare DM, Collins JE, McCann OT, Young BD, Debernardi S, Mott R, Dunham I, Carter NP. Replication timing of the human genome. Hum Mol Genet 2004; 13:191-202; PMID:14645202; http://dx.doi.org/10.1093/hmg/ddh016
19. Jeon Y, Bekiranov S, Karnani N, Kapranov P, Ghosh S, MacAlpine D, Lee C, Hwang DS, Gingeras TR, Dutta A. Temporal profile of replication of human chromosomes. Proc Natl Acad Sci U S A 2005; 102:6419-24; PMID:15845769; http://dx.doi.org/10.1073/pnas.0405088102
20. French S. Consequences of replication fork movement through transcription units in vivo. Science 1992; 258:1362-5; PMID:1455232; http://dx.doi.org/10.1126/science.1455232
21. Deshpande AM, Newlon CS. DNA replication fork pause sites dependent on transcription. Science 1996; 272:1030-3; PMID:8638128; http://dx.doi.org/10.1126/science.272.5264.1030
22. Azvolinsky A, Giresi PG, Lieb JD, Zakian VA. Highly transcribed RNA polymerase II genes are impediments to replication fork progression in Saccharomyces cerevisiae. Molecular Cell 2009; 34:722-34; PMID:19560424; http://dx.doi.org/10.1016/j.molcel.2009.05.022
23. Coffman FD, He M, Diaz ML, Cohen S. DNA replication initiates at different sites in early and late S phase within human ribosomal RNA genes. Cell Cycle 2005; 4:1223-6; PMID:16082215; http://dx.doi.org/10.4161/cc.4.9.1961
24. Larsson E, Sander C, Marks D. mRNA turnover rate limits siRNA and microRNA efficacy. Mol Syst Biol 2010; 6:433; PMID:21081925
25. Subramanian A, Tamayo P, Mootha VK, Mukherjee S, Ebert BL, Gillette MA, Paulovich A, Pomeroy SL, Golub TR, Lander ES, et al. Gene set enrichment

analysis: a knowledge-based approach for interpreting genome-wide expression profiles. Proc Nat Acad Sci U S A 2005; 102:15545-50; PMID:16199517; http://dx.doi.org/10.1073/pnas.0506580102

26. Mootha VK, Lindgren CM, Eriksson KF, Subramanian A, Sihag S, Lehar J, Puigserver P, Carlsson E, Ridderstrale M, Laurila E, et al. PGC-1alpha-responsive genes involved in oxidative phosphorylation are coordinately downregulated in human diabetes. Nature genetics 2003; 34:267-73; PMID:12808457; http://dx.doi.org/10.1038/ng1180

27. Ashburner M, Ball CA, Blake JA, Botstein D, Butler H, Cherry JM, Davis AP, Dolinski K, Dwight SS, Eppig JT, et al. Gene ontology: tool for the unification of biology. The Gene Ontology Consortium. Nature genetics 2000; 25:25-9; PMID:10802651; http://dx.doi.org/10.1038/75556